Journal of
Applied and Computational Mechanics

Shahid Chamran
University of Ahvaz

A Nonlinear Lagrangian Model for Plane Frames Pre-design

Omar S. Rojas[1,2], Alex X. Jerves[1,2,3], David A. Medina[2]

[1]Facultad de Ingeniería, Universidad Católica de Cuenca, Avenida de las Américas y Humbolt, Cuenca, Azuay, Ecuador, Email: omarsrc@gmail.com (O.S.R.)
[2]Fundación INSPIRE, INS7RE, Quito, Pichincha, Ecuador, Email: ajerves@inspire.ec (A.X.J.); dmedina@inspire.ec (D.A.M.)
[3]Advanced Numerical Modeling, Norwegian Geotechnical Institute, Oslo, Norway, Email: alex.xavier.jerves@ngi.no

Abstract. We propose a nonlinear lagrangian model that takes into account the dynamic interactions between the soil and a n-storey plane frame, which may be subjected to a seismic excitation through the soil. First, the interaction of the soil with the structure is modeled through a combination of springs and dampers representing the characteristics of the soil. In this model, the masses and stiffnesses of the structure elements are condensed to facilitate the analysis. Second, the Euler-Lagrange equations of the system are formulated and generalized for n floors. Third, these equations are discretized using the finite difference method to solve them using the Newton-Raphson method at each time step, during and after the seismic excitation, thus, determining the positions of each concentrated mass of the system. In addition, a linearization of the governing equations is performed in order to compare these results with those of the nonlinear model. Finally, the nonlinear model is used for the analysis of a 10-storey building, which has already been designed for linear geometric and material behaviors. For this analysis, the corrected acceleration record of the 2016 Pedernales (Ecuador) earthquake is used.

Keywords: soil-structure interaction, lagrangian model, seismic excitation, large displacements.

1. Introduction

In the seismic resistant analysis of buildings, one of the fundamental parts corresponds to the analysis of the soil where the building will be supported, since the design of the foundation will depend on this. For this reason, the study of the soil-structure interaction is fundamental for an adequate seismic resistant design. For example, the so-called "stick models" have failed in an adequate prediction of the structural behavior under a given seismic excitation [1], since the foundations are considered as rigid plates, i.e., the effects of soil-structure interaction are completely omitted [2].

At the end of the 1970s, with the appearance of the first commercial computers, authors such as Chopra [3] and Whitman [4], put more emphasis on the incorporation of the interaction between soil and the structure in the analysis of structures subjected to a seismic excitation [5, 6]. The effect of the soil on the structure has an important effect on the dynamic behavior of the structure, which is reflected in an increase in the fundamental period, as well as in an increase in the damping of the system compared to the fixed base model that does not consider interactions with the ground [8, 7].

On the other hand, it is commonly assumed that the soil-structure interaction is detrimental to the structural response of buildings, which is not entirely true. In some cases, the consideration of soil-structure interaction can be favorable. This is the case of rigid structures, which work only within the elastic range. In rigid structures, the consideration of soil-structure interaction will generally be beneficial in the mechanical response of the structure.

Under the considerations mentioned so far, it is clear the importance of the soil-structure interaction at the moment of carrying out a seismic resistant design. A precise knowledge of the soil-structure interaction and how it can affect the response of the building under a seismic event can contribute to safer designs, while, optimizing materials and resources. Within the field of seismic-resistant design, in recent years, more emphasis has been placed on the analysis of soil interaction with the structure. However, most of the methods assume a regime of small ground deformations and displacements. In the best case, some models assume the soil-structure interaction as a linear behavior in each of the parts.

Nonetheless, in general, the methods used in the modeling of nonlinear deformations in structures (where the soil-structure interaction is included) are not simple nor user-friendly enough to be assumed as a base for design in engineering [9, 10, 11, 12, 13, 14]. This is why the use of Lagrangian mechanics theory allows a greater generalization and abstraction of structural models than its Newtonian counterpart [15].

The study of nonlinear dynamic behavior may allow to create a reliable and practical physical-mathematical model that simplifies the interpretation of the influence of the soil on the structure.

2. Physical-mathematical model

The problem to be analyzed consists of a n-storey plane frame that is subjected to a horizontal movement at its base due to a seismic force (see Fig. 1). The model starts from the idealization of the frame by concentrating the mass of each level, which is
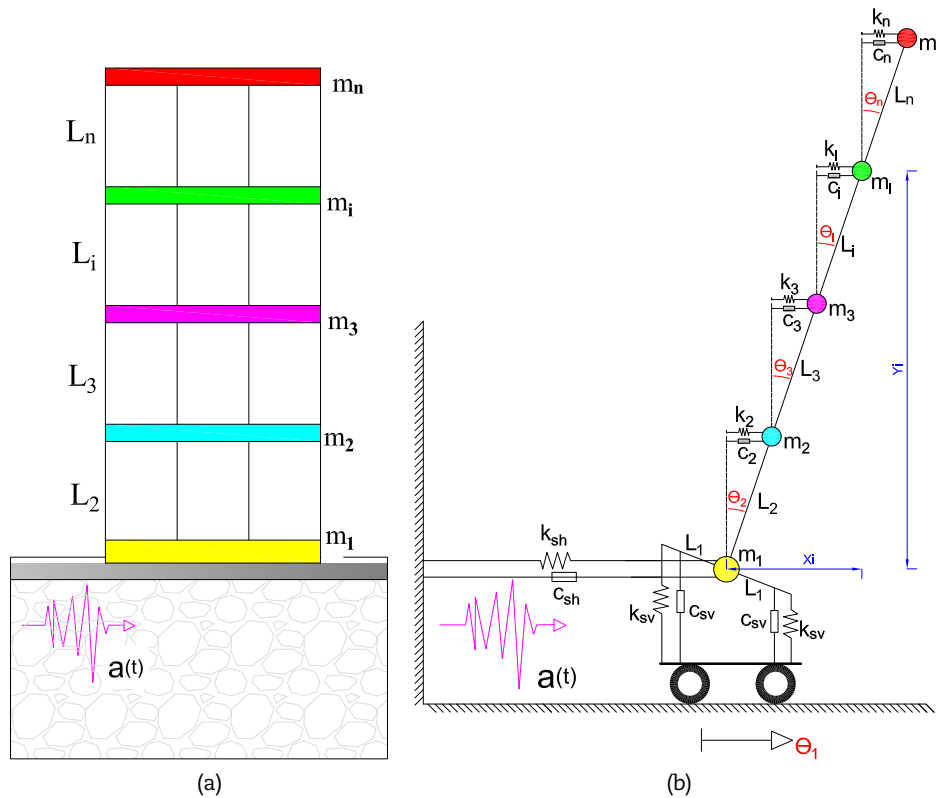
Fig. 1. Physical-mathematical model of a n-storey plane frame: a) plane portal frame of an n-storey building with slab foundation, where L_i is the height of the i-th floor and m_i is the mass of each floor. The building is subjected to a seismic event, applied to its base (foundation slab), b) mathematical physical model of the nonlinear mechanical behavior of the flat portal frame (a) due to large displacements, where k_i is the stiffness of the i-th floor. Moreover, c_i is the damping constant of the i-th floor. The interaction of the soil with the structure is modeled by the system of springs and dampers at the base, connected to the mass m_1 corresponding to the foundation slab. The external forcing $a(t)$ is applied to the foundation by means of the aforementioned system of springs and dampers representing the soil underneath the base slab.

supported by a "single column" without mass and with effective stiffness equivalent to that of the columns between consecutive levels [15] (see Fig. 1 (b)). Hence, such stiffness is a function of the column cross-sections' geometric characteristics, the material of the portalized system, and the type of restraint at the nodes (e.g., beam-column joints).

On the other hand, the interaction between soil and the structure is modeled taking into account previous research such as the work by Gazetas and Wolf [16, 17]. They proposed to model the behavior of the ground as a system with one degree of freedom, idealized by springs on an rigid deck representing the bearing ground. Similarly, to model the dissipative capacity of the system, dampers [18] are used, viscoelastic behavior of the columns and the soil represented by a Kelvin-Voigt model for each mass are also assumed, where the spring and the damper act in parallel [19] as shown in Fig. 1 (b).

3. Model application of Lagrangian mechanics

The complexity of the model shown in Fig. 1 (b) is in its generalization for n floors, hence the use of traditional methods in structural engineering, such as those based on Newtonian mechanics can become tedious [20]. This is the reason for the need to use equivalent formulations, but with greater advantages that can formulate mechanical phenomena in a mathematical way such as that offered by Lagrangian mechanics, based on variational principles [21].

3.1 Kinetic energy of the system

The geometric position of each mass m_i in Fig. 1 (b) is given by expressions (1), which are a function of the degrees of freedom θ_i. Note that, θ_1 represents the horizontal displacement, and that θ_i for $i = 2 : n$ represents the rotational degrees of freedom of the system. Then,

$$
\begin{cases}
x_i = \theta_1 + \displaystyle\sum_{j=2}^{i} L_j \sin \theta_j \\[3mm]
y_i = \displaystyle\sum_{j=2}^{i} L_j \cos \theta_j
\end{cases}
\tag{1}
$$

where the velocities of the masses m_i in each Cartesian coordinate are obtained from the time derivative of equations (1) and given by equations (2):

$$\begin{cases} \dot{x_i} = \dot{\theta}_1 + \sum_{j=2}^{i} L_j \dot{\theta}_j \cos \theta_j \\ \\ \dot{y_i} = - \sum_{j=2}^{i} L_j \dot{\theta}_j \sin \theta_j \end{cases} \qquad (2)$$

Thus, from equations (2), the tangential velocity is given by:

$$v_i^2 = \dot{x_i}^2 + \dot{y_i}^2$$

Then, the kinetic energy T of the system is the sum of the kinetic energy of each mass m_i [22], as follows:

$$T = \frac{1}{2} \sum_{i=1}^{n} m_i \left(\dot{x_i}^2 + \dot{y_i}^2 \right)$$

and substituting equations (2) into the last equation, we end up with:

$$T = \frac{1}{2} \sum_{i=1}^{n} m_i \left[\left(\dot{\theta}_1 + \sum_{j=2}^{i} L_j \dot{\theta}_j \cos \theta_j \right)^2 + \left(\sum_{j=2}^{i} L_j \dot{\theta}_j \sin \theta_j \right)^2 \right] \qquad (3)$$

3.2 Potential energy of the system

The potential energy of the system is the sum of the potential energies of each mass, in turn, the potential energy of each mass is the sum of the gravitational potential energy and the elastic potential energy of the springs. The model synthesized graphically in Fig. 1 (b) takes into account the nondissipative interaction of the soil with the structure through springs, such that, for m_1 (the foundation's mass) the potential energy is given by:

$$V_1 = \frac{1}{2} k_{sh} \theta_1^2 + (\frac{1}{2} k_{sv} (L_1 \sin \theta_1)^2)2 = \frac{1}{2} k_{sh} \theta_1^2 + k_{sv} L_1^2 \sin^2 \theta_1 \qquad (4)$$

where k_{sh} is the horizontal stiffness of soil, k_{sv} the vertical stiffness of soil, L_1 half of the foundation's horizontal length (see Fig. 1), and θ_1 the horizontal rotation of mass m_1. Similarly, the potential energy of the masses m_i for $i = 2 : n$ is given by:

$$V_i = \frac{1}{2} k_i L_i^2 sin^2 \theta_i + m_i g \sum_{j=2}^{i} L_j \cos \theta_j \qquad (5)$$

where, L_i is the floor length and θ_i the angular displacement for $i = 2 : n$. Finally, the potential energy of the system is given by:

$$V = \frac{1}{2} k_{sh} \theta_1^2 + k_{sv} L_1^2 \sin^2 \theta_1 + \sum_{i=2}^{n} \frac{1}{2} k_i L_i^2 sin^2 \theta_i + \sum_{i=2}^{n} m_i g \sum_{j=2}^{i} L_j \cos \theta_j \qquad (6)$$

3.3 Lagrangian model of the system

Once the total potential energy (6) and the total kinetic energy of the system (3) have been computed, the Lagrangian of the system $\mathcal{L} = T - V$ ends up as follows:

$$\mathcal{L} = \frac{1}{2} \sum_{i=1}^{n} m_i \left[\left(\dot{\theta}_1 + \sum_{j=2}^{i} L_j \dot{\theta}_j \cos \theta_j \right)^2 + \left(\sum_{j=2}^{i} L_j \dot{\theta}_j \sin \theta_j \right)^2 \right] - \frac{1}{2} k_{sh} \theta_1^2$$

$$- k_{sv} L_1^2 \sin^2 \theta_1 - \frac{1}{2} \sum_{i=2}^{n} k_i L_i^2 sin^2 \theta_i - \sum_{i=2}^{n} m_i g \sum_{j=2}^{i} L_j \cos \theta_j$$

From this Lagrangian, n Euler - Lagrange equations, one for each degree of freedom of the structure θ_i, which satisfies the Stationary-action principle [22], are obtained.

$$\frac{\partial \mathcal{L}}{\partial \theta_i} - \frac{d}{dt} \left(\frac{\partial \mathcal{L}}{\partial \dot{\theta}_i} \right) = \sum F_{dis-m_i} \qquad (7)$$

where, the right-hand term of the equation corresponds to the dissipative forces in the system, from the dampers with a linear viscous model [25], given by:

$$F_{dis-m_i} = -c_i \dot{x}_i$$

here, c_i is the damping coefficient and $\dot{x}_i$ is given by expression (2). Finally, from the Lagrangian equations (7) we get:

For $q = 1$,

$$\left(\sum_{i=1}^{n} m_i \right) \ddot{\theta}_1 + \sum_{j=2}^{n} \left(\sum_{i=j}^{n} m_i \right) L_j \cos \theta_j \ddot{\theta}_j - \sum_{j=2}^{n} \left(\sum_{i=j}^{n} m_i \right) L_j \sin \theta_j \dot{\theta}_j^2 + k_{sh} \theta_1 + c_{sh} \dot{\theta}_1 = f(t) \qquad (8)$$

For $q = 2$,

$$\left(\sum_{i=2}^{n} m_i\right) L_2 \cos \theta_2 \ddot{\theta_1} + \left(\sum_{i=2}^{n} m_i\right) L_2^2 \ddot{\theta_2} + \sum_{j=3}^{n} \left(\sum_{i=j}^{n} m_i\right) L_2 L_j \cos\left(\theta_2 - \theta_j\right) \ddot{\theta_j}$$

$$+ \sum_{j=3}^{n} \left(\sum_{i=j}^{n} m_i\right) L_2 L_j \sin\left(\theta_2 - \theta_j\right) \dot{\theta_j}^2 + k_{sv} L_1^2 \sin\left(2\theta_2\right) + \frac{1}{2} k_2 L_2^2 \sin\left(2\theta_2\right) \tag{9}$$

$$- \left(\sum_{i=2}^{n} m_i\right) g L_2 \sin \theta_2 + 2 c_{sv} L_1 \cos \theta_2 \dot{\theta_2} + c_2 \dot{\theta_1} + c_2 L_2 \cos \theta_2 \dot{\theta_2} = 0$$

For $q = 3 : n$,

$$\left(\sum_{i=q}^{n} m_i\right) L_q \cos \theta_q \ddot{\theta_1} + \sum_{\substack{j=2 \\ j \neq q}}^{n} \left(\begin{cases} j < q \Rightarrow \left(\displaystyle\sum_{i=q}^{n} m_i\right) \\ j > q \Rightarrow \left(\displaystyle\sum_{i=j}^{n} m_i\right) \end{cases} \right) L_q L_j \cos\left(\theta_q - \theta_j\right) \ddot{\theta_j}$$

$$+ \left(\sum_{i=q}^{n} m_i\right) L_q^2 \ddot{\theta_q} + \sum_{\substack{j=2 \\ j \neq q}}^{n} \left(\begin{cases} j < q \Rightarrow \left(\displaystyle\sum_{i=q}^{n} m_i\right) \\ j > q \Rightarrow \left(\displaystyle\sum_{i=j}^{n} m_i\right) \end{cases} \right) L_q L_j \sin(\theta_q - \theta_j) \dot{\theta_j}^2 \tag{10}$$

$$+ \frac{1}{2} k_q L_q^2 \sin(2\theta_q) - \left(\sum_{i=q}^{n} m_i\right) g L_q \sin \theta_q + c_q \dot{\theta_1} + \sum_{j=2}^{q} c_q L_j \cos \theta_j \dot{\theta_j} = 0$$

where q is the equation number within the system of n equations for $q = 1 : n$. The first two equations, $q = 1$ and $q = 2$, have a different generalization than the others because the masses m_1 and m_2 are intrinsically in contact with the soil, and where c_{sh} and c_{sv} represent the horizontal and vertical damping coefficients of the soil, respectively.

On the other hand, note that on the right-hand side of equation (8) is a function of time $f(t)$ representing an external force term given, that (in this model) is given, for example, by a seismic excitation acting on the bearing ground with mass m_1. In the case that one wants to apply other external forces, for instance, the forces exerted on the structures by the action of the wind, it would be enough to add to the right side of the equality of the equations (9) and/or (10) (the function of the corresponding external forces) to the equations corresponding to the upper masses.

4. Numerical solution of the system

Since this is a system of highly nonlinear ordinary differential equations it is impossible to solve it analytically. The nonlinearity is clearly of geometric origin, due to large deformations produced by an external forces in the soil. Hence, the only way to solve the system given by the numerical expressions (8), (9), and (10) [23]. Specifically, here we use the finite difference method for this purpose.

4.1 System discretization by the finite difference method

In this case, we adopt for the first derivatives in a forward finite difference scheme given by:

$$\dot{\theta_i} = \frac{\theta_{i,p+1} - \theta_{i,p}}{\Delta t} + O\left(\Delta t\right) \tag{11}$$

In addition, a central finite difference scheme is used for the second derivatives:

$$\ddot{\theta_i} = \frac{\theta_{i,p+1} - 2\theta_{i,p} + \theta_{i,p-1}}{\Delta t^2} + O\left(\Delta t^2\right) \tag{12}$$

Substituting the equations (11) and (12) into the expressions (8), (9) and (10) result in the following system of equations:
For $q = 1$,

$$\left(\sum_{i=1}^{n} m_i\right) \left(\theta_{1,p+1} - 2\theta_{1,p} + \theta_{1,p-1}\right) - \sum_{j=2}^{n} \left(\sum_{i=j}^{n} m_i\right) L_j \sin \theta_{j,p} \left(\theta_{j,p+1} - \theta_{j,p}\right)^2$$

$$+ \sum_{j=2}^{n} \left(\sum_{i=j}^{n} m_i\right) L_j \cos \theta_{j,p} \left(\theta_{j,p+1} - 2\theta_{j,p} + \theta_{j,p-1}\right) + k_{sh} \theta_{1,p} \Delta t^2 \tag{13}$$

$$+ c_{sh} \left(\theta_{1,p+1} - \theta_{1,p}\right) \Delta t - f\left(t\right) \Delta t^2 = 0$$

For $q = 2$,

$$\left(\sum_{i=2}^{n} m_i\right) L_2 \cos\theta_{2,p} \left(\theta_{1,p+1} - 2\theta_{1,p} + \theta_{1,p-1}\right) + \left(\sum_{i=2}^{n} m_i\right) L_2^2 \left(\theta_{2,p+1} - 2\theta_{2,p} + \theta_{2,p-1}\right)$$

$$+ \sum_{j=3}^{n} \left(\sum_{i=j}^{n} m_i\right) L_2 L_j \cos\left(\theta_{2,p} - \theta_{j,p}\right) \left(\theta_{j,p+1} - 2\theta_{j,p} + \theta_{j,p-1}\right)$$

$$+ \sum_{j=3}^{n} \left(\sum_{i=j}^{n} m_i\right) L_2 L_j \sin\left(\theta_{2,p} - \theta_{j,p}\right) \left(\theta_{j,p+1} - \theta_{j,p}\right)^2 + k_{sv} L_1^2 \sin\left(2\theta_{2,p}\right) \Delta t^2 \qquad (14)$$

$$+ \frac{1}{2} k_2 L_2^2 \sin\left(2\theta_{2,p}\right) \Delta t^2 - \left(\sum_{i=2}^{n} m_i\right) g L_2 \sin\theta_{2,p} \Delta t^2 + 2 c_{sv} L_1 \cos\theta_{2,p} \left(\theta_{2,p+1} - \theta_{2,p}\right) \Delta t$$

$$+ c_2 \left(\theta_{1,p+1} - \theta_{1,p}\right) \Delta t + c_2 L_2 \cos\theta_{2,p} \left(\theta_{2,p+1} - \theta_{2,p}\right) \Delta t = 0$$

For $q = 3 : n$,

$$\left(\sum_{i=q}^{n} m_i\right) L_q \cos\theta_{q,p} \left(\theta_{1,p+1} - 2\theta_{1,p} + \theta_{1,p-1}\right) + \left(\sum_{i=q}^{n} m_i\right) L_q^2 \left(\theta_{q,p+1} - 2\theta_{q,p} + \theta_{q,p-1}\right)$$

$$+ \sum_{\substack{j=2 \\ j\neq q}}^{n} \left(\begin{matrix} j < q \Rightarrow \left(\sum_{i=q}^{n} m_i\right) \\ j > q \Rightarrow \left(\sum_{i=j}^{n} m_i\right) \end{matrix}\right) L_q L_j \cos\left(\theta_{q,p} - \theta_{j,p}\right) \left(\theta_{j,p+1} - 2\theta_{j,p} + \theta_{j,p-1}\right)$$

$$+ \sum_{\substack{j=2 \\ j\neq q}}^{n} \left(\begin{matrix} j < q \Rightarrow \left(\sum_{i=q}^{n} m_i\right) \\ j > q \Rightarrow \left(\sum_{i=j}^{n} m_i\right) \end{matrix}\right) L_q L_j \sin\left(\theta_{q,p} - \theta_{j,p}\right) \left(\theta_{j,p+1} - \theta_{j,p}\right)^2 \qquad (15)$$

$$+ \frac{1}{2} k_q L_q^2 \sin(2\theta_{q,p}) \Delta t^2 - \left(\sum_{i=q}^{n} m_i\right) g L_q \sin\theta_{q,p} \Delta t^2 + c_q \left(\theta_{1,p+1} - \theta_{1,p}\right) \Delta t$$

$$+ \sum_{j=2}^{q} c_q L_j \cos\theta_{j,p} \left(\theta_{j,p+1} - \theta_{j,p}\right) \Delta t = 0$$

Note that equations (13), (14), and (15), form a system of n nonlinear algebraic equations with n unknowns subject to initial conditions, which has to be solved for each time step (denoted in the discretized variables by the subscript p).

4.2 Numerical solution to the system of discretized equations

In order to solve the system of equations given by (13), (14) and (15), it is necessary to discretize the initial conditions [23], in other words:

$$\begin{cases} \theta_{1,p-1} = \alpha_1 & \dot{\theta}_{1,p-1} = V_1 \\ \theta_{2,p-1} = \alpha_2 & \dot{\theta}_{2,p-1} = V_2 \\ \quad \ldots & \quad \ldots \\ \theta_{i,p-1} = \alpha_i & \dot{\theta}_{i,p-1} = V_i \\ \quad \ldots & \quad \ldots \\ \theta_{n,p-1} = \alpha_n & \dot{\theta}_{n,p-1} = V_n \end{cases}$$

where, the values of α_i and V_i represent the initial conditions of the kinematic state of the structure and p is the time index ranging from 2 to m. Thus, for the discretization of $\dot{\theta}_{i,p-1}$ we use the progressive finite difference scheme (11), from which we obtain:

$$\begin{cases} V_1 = \dfrac{\theta_{1,p} - \theta_{1,p-1}}{\Delta t} \Rightarrow \theta_{1,p} = V_1 . \Delta_t + \theta_{1,p-1} \\[2mm] V_2 = \dfrac{\theta_{2,p} - \theta_{2,p-1}}{\Delta t} \Rightarrow \theta_{2,p} = V_2 . \Delta_t + \theta_{2,p-1} \\[1mm] \ldots \\ V_i = \dfrac{\theta_{i,p} - \theta_{i,p-1}}{\Delta t} \Rightarrow \theta_{i,p} = V_i . \Delta_t + \theta_{i,p-1} \\[1mm] \ldots \\ V_n = \dfrac{\theta_{n,p} - \theta_{n,p-1}}{\Delta t} \Rightarrow \theta_{n,p} = V_n . \Delta_t + \theta_{n,p-1} \end{cases} \qquad (16)$$

with, $\theta_{i,p-1} = 0 \rightarrow i = 1....n$. Then, when combining the system of nonlinear algebraic equations (13), (14) and (15) with the discretized initial conditions (16), one must solve such system for each time step to obtain the values of $\theta_{i,p+1}$ for $p = 2 : m$ time steps, where m represents the number of time steps to be analyzed with Δt increments.

Finally, the Newton-Raphson numerical method [24] is used to solve the system of equations given by the expressions (13), (14) and (15) subject to the initial conditions (16). The associated iterative process is given by:

$$
\begin{Bmatrix} \theta_{1,p+1} \\ \theta_{2,p+1} \\ \cdots \\ \theta_{i,p+1} \\ \cdots \\ \theta_{n,p+1} \end{Bmatrix}^{(k+1)} \approx \begin{Bmatrix} \theta_{1,p} \\ \theta_{2,p} \\ \cdots \\ \theta_{i,p} \\ \cdots \\ \theta_{n,p} \end{Bmatrix}^{(k)} - \begin{bmatrix} J_{1,1} & J_{1,2} & \cdots & J_{1,j} & \cdots & J_{1,n} \\ J_{2,1} & J_{2,2} & \cdots & J_{2,j} & \cdots & J_{2,n} \\ \cdots & \cdots & \cdots & \cdots & \cdots & \cdots \\ J_{i,1} & J_{i,2} & \cdots & J_{i,j} & \cdots & J_{i,n} \\ \cdots & \cdots & \cdots & \cdots & \cdots & \cdots \\ J_{n,1} & J_{n,2} & \cdots & J_{n,j} & \cdots & J_{n,n} \end{bmatrix}^{(k)} \begin{Bmatrix} f_1 \\ f_2 \\ \cdots \\ f_i \\ \cdots \\ f_n \end{Bmatrix}^{(k)}
\tag{17}
$$

where, k denotes the iteration number. In this case, by the nature of the iterative method, it is necessary to set a tolerance for the solution. In addition, f_i is the residual of each of the algebraic equations (13), (14) and (15), and $J_{i,j}$ is the Jacobian of the system given by:

$$
J_{i,j} = \left. \frac{\partial f_i}{\partial \theta_{j,p+1}} \right|^{(k)}
\tag{18}
$$

Thus, from equations (13), (14), (15) and (18) we obtain:
For row 1, column 1:

$$
J_{1,1} = \sum_{i=1}^{n} m_i + c_{sh}\Delta t
$$

Row 1, column j, for $j = 2 : n$:

$$
J_{1,j} = \left(\sum_{i=j}^{n} m_i \right) L_j \cos\theta_{j,p} - 2 \left(\sum_{i=j}^{n} m_i \right) L_j \sin\theta_{j,p} \left(\theta_{j,p+1} - \theta_{j,p} \right)
$$

Row 2, column 1:

$$
J_{2,1} = \left(\sum_{i=2}^{n} m_i \right) L_2 \cos\theta_{2,p} + c_2\Delta t
$$

Row 2, column 2:

$$
J_{2,2} = \left(\sum_{i=2}^{n} m_i \right) L_2^2 + (2c_{sv}L_1 + c_2 L_2)\cos\theta_{2,p}\Delta t
$$

Row 2, column j, for $j = 3 : n$:

$$
J_{2,j} = \left(\sum_{i=j}^{n} m_i \right) L_2 L_j \cos\left(\theta_{2,p} - \theta_{j,p} \right) + 2 \left(\sum_{i=j}^{n} m_i \right) L_2 L_j \sin\left(\theta_{2,p} - \theta_{j,p} \right)\left(\theta_{j,p+1} - \theta_{j,p} \right)
$$

Row q, for $q = 3 : n$, column 1:

$$
J_{q,1} = \left(\sum_{i=q}^{n} m_i \right) L_q \cos\theta_{q,p} + c_q\Delta t
$$

Row q, for $q = 3 : n$, column j, for $j = 2 : n$ and $j \neq q$:

$$
J_{q,j} = \left(\begin{matrix} j < q \Rightarrow \left(\sum_{i=q}^{n} m_i \right) \\ j > q \Rightarrow \left(\sum_{i=j}^{n} m_i \right) \end{matrix} \right) L_q L_j \cos\left(\theta_{q,p} - \theta_{j,p} \right)
$$

$$
+ 2 \left(\begin{matrix} j < q \Rightarrow \left(\sum_{i=q}^{n} m_i \right) \\ j > q \Rightarrow \left(\sum_{i=j}^{n} m_i \right) \end{matrix} \right) L_q L_j \sin(\theta_{q,p} - \theta_{j,p})\left(\theta_{j,p+1} - \theta_{j,p} \right)
$$

$$
+ c_q L_j \cos\theta_{j,p}\Delta t = 0
$$

Row q, column q, for $q = 3 : n$:

$$
J_{q,q} = \left(\sum_{i=q}^{n} m_i \right) L_q^2 + c_q L_q \cos\theta_{q,p}\Delta t
$$

It is worth noticing that each term from the Jacobian matrix has also been generalized for n floors. Then, the position of each mass m_i is obtained by solving the system given by equations (13), (14) and (15) for each time step with a Newton-Raphson scheme.

Finally, Fig. 2 presents a flow diagram of the numerical solution for the mathematical-physical model in Fig. 1 (b), represented by equations (8), (9) and (10), and which are subjected to the initial conditions (16).
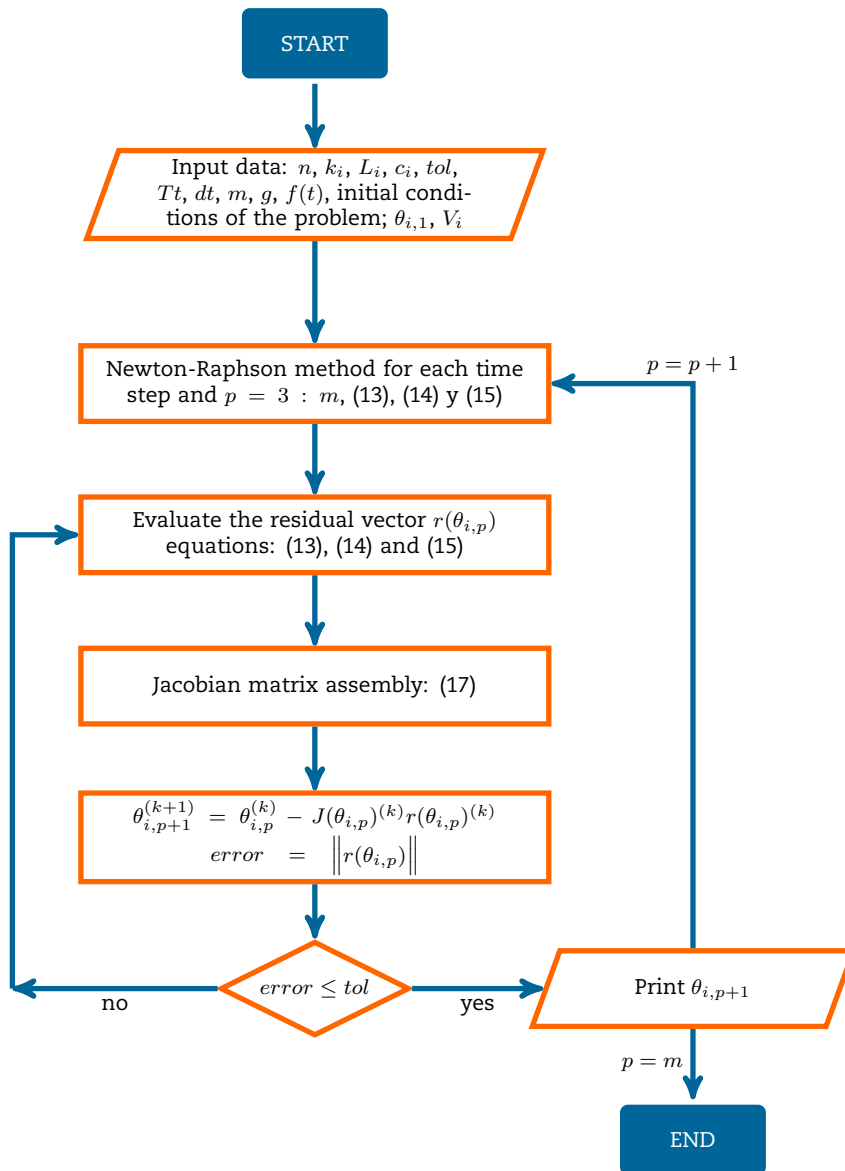
Fig. 2. Flowchart of the numerical solution for a nonlinear lagrangian model of a n-storey plane frame.

5. Model linearization

In this section, equations (14), (15), and (16) are linearized. In practice, this implies assuming that the structure will be subjected exclusively to small deformations and displacements, which are usually within the norms of structural design in civil engineering.

Mathematically, this implies that one can safely assume that the angles of the rotational degrees of freedom of the system are small (i.e. $\theta_i \simeq 0$), which, in turn, imply that:

$$
\begin{cases}
\sin \theta_i \simeq \theta_i \\[2mm]
\cos \theta_i \simeq 1
\end{cases}
$$

Furthermore, small rotation angles in a structure with high stiffness elements also imply that the angular velocities of the rotational degrees of freedom of the system can also be assumed to be "small", hence:

$$
\dot{\theta_i}^2 \simeq 0
$$

Thus, applying these assumptions to the expressions (8), (9) and (10), we get:
For $q = 1$,

$$
\left(\sum_{i=1}^{n} m_i\right) \ddot{\theta}_1 + \sum_{j=2}^{n} \left(\sum_{i=j}^{n} m_i\right) L_j \ddot{\theta}_j + k_{sh}\theta_1 + c_{sh}\dot{\theta}_1 = 0 \tag{19}
$$

For $q = 2$,

$$
\left(\sum_{i=2}^{n} m_i\right) L_2 \ddot{\theta}_1 + \left(\sum_{i=2}^{n} m_i\right) L_2^2 \ddot{\theta}_2 + \sum_{j=3}^{n} \left(\sum_{i=j}^{n} m_i\right) L_2 L_j \ddot{\theta}_j
$$

$$
+ 2k_{sv}L_1^2\theta_2 + k_2 L_2^2\theta_2 - \left(\sum_{i=2}^{n} m_i\right) g L_2 \theta_2 + 2c_{sv}L_1\dot{\theta}_2 + c_2\dot{\theta}_1 + c_2 L_2\dot{\theta}_2 = 0 \tag{20}
$$

For $q = 3 : n$,

$$
\left(\sum_{i=q}^{n} m_i\right) L_q \ddot{\theta}_1 + \sum_{\substack{j=2 \\ j \neq q}}^{n} \left(\begin{array}{l} j < q \Rightarrow \left(\displaystyle\sum_{i=q}^{n}\right) \\[4mm] j > q \Rightarrow \left(\displaystyle\sum_{i=j}^{n}\right) \end{array}\right) L_q L_j \ddot{\theta}_j + \left(\sum_{i=q}^{n} m_i\right) L_q^2 \ddot{\theta}_q + k_q L_q^2 \theta_q
$$

$$
- \left(\sum_{i=q}^{n} m_i\right) g L_q \theta_q + c_q \dot{\theta}_1 + \sum_{j=2}^{q} c_q L_j \theta_j \dot{\theta}_j = 0 \tag{21}
$$

Note that in this system of n ordinary differential equations with n unknowns, i.e., $\theta_i(t)$, given by the expressions (19), (20) and (21), all the differential equations are linear. We compute the numerical solution using finite differences and the expressions (11) and (12) as previously done to solve the nonlinear model, from which we obtain:
For $q = 1$,

$$
\left(\left(\sum_{i=1}^{n} m_i\right) + c_{sh}\Delta t\right) \theta_{1,p+1} + \sum_{j=2}^{n} \left(\sum_{i=j}^{n} m_i\right) L_j \theta_{j,p+1} = \left(\sum_{i=1}^{n} m_i\right) (2\theta_{1,p} - \theta_{1,p-1})
$$

$$
+ \sum_{j=2}^{n} \left(\sum_{i=j}^{n} m_i\right) L_j (2\theta_{j,p} - \theta_{j,p-1}) + \left(c_{sh}\Delta t - k_{sh}\Delta t^2\right) \theta_{1,p} - f(i) \tag{22}
$$

For $q = 2$,

$$
\left(\left(\sum_{i=2}^{n} m_i\right) L_2 + c_2\Delta t\right) \theta_{1,p+1} + \left(\left(\sum_{i=2}^{n} m_i\right) L_2 + 2c_{sv}L_1\Delta t + c_2 L_2\Delta t\right) \theta_{2,p+1}
$$

$$
+ \sum_{j=3}^{n} \left(\sum_{i=j}^{n} m_i\right) L_2 L_j \theta_{j,p+1} = \left(\sum_{i=2}^{n} m_i\right) L_2 (2\theta_{1,p} - \theta_{1,p-1})
$$

$$
+ \left(\sum_{i=2}^{n} m_i\right) L_2^2 (2\theta_{2,p} - \theta_{2,p-1}) + \sum_{j=3}^{n} \left(\sum_{i=j}^{n} m_i\right) L_2 L_j (2\theta_{j,p} - \theta_{j,p-1}) + c_2\Delta t\theta_{1,p}
$$

$$
+ \left((2c_{sv}L_1 + c_2 L_2) - \left(2k_{sv}L_1^2 + k_2 L_2^2 - \left(\sum_{i=2}^{n} m_i\right) g L_2\right)\Delta t\right)\Delta t\theta_{2,p} \tag{23}
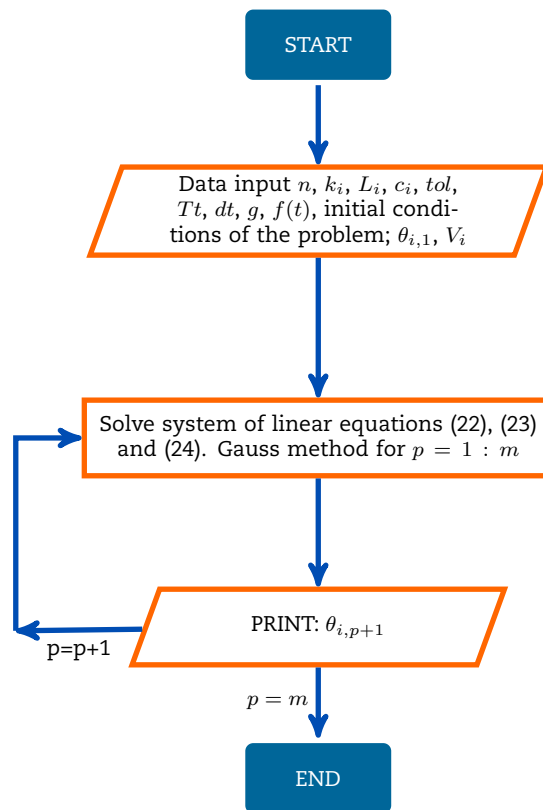$$

Fig. 3. Flowchart of the numerical solution for the linear Lagrangian model of a n-storey plane frame.

For $q = 3 : n$,

$$
\left(\left(\sum_{i=q}^{n} m_i\right) L_q + c_q \Delta t\right) \theta_{1,p+1} + \left(\left(\sum_{i=q}^{n} m_i\right) L_q^2 + c_q L_q \Delta t\right) \theta_{q,p+1}
$$

$$
+ \left(\sum_{\substack{j=2 \\ j \neq q}}^{n} \left(\begin{matrix} j < q \Rightarrow \left(\sum_{i=q}^{n} m_i\right) \\ j > q \Rightarrow \left(\sum_{i=j}^{n} m_i\right) \end{matrix}\right) L_q L_j + \sum_{j=2}^{q-1} c_q L_j \Delta t\right) \theta_{j,p+1} = \left(\sum_{i=q}^{n} m_i\right) L_q \left(2\theta_{1,p} - \theta_{1,p-1}\right)
$$

$$
+ \left(\sum_{i=q}^{n} m_i\right) L_q^2 \left(2\theta_{q,p} - \theta_{q,p-1}\right) + \left(\sum_{\substack{j=2 \\ j \neq q}}^{n} \left(\begin{matrix} j < q \Rightarrow \left(\sum_{i=q}^{n} m_i\right) \\ j > q \Rightarrow \left(\sum_{i=j}^{n} m_i\right) \end{matrix}\right)\right) L_q L_j \left(2\theta_{j,p} - \theta_{j,p-1}\right)
$$

$$
+ c_q \Delta t \theta_{1,p-1} + \sum_{j=2}^{q} c_q L_j \Delta t \theta_{j,p} + \left(\left(\sum_{i=q}^{n} m_i\right) g L_q - k_q L_q^2\right) \Delta t^2 \theta_{q,p} \tag{24}
$$

Finally, Fig. 3 shows a flow diagram of the numerical solution for the linearized model in Fig. 1 (b), represented by equations (22), (23) and (24), and which are subjected to the initial conditions (16).

6. A 10-storey building design evaluation

In this section, the developed model is applied to the 10-storey building shown in Fig. 4.

Figure 5 (a) represents the central frame of the building with its geometry and the effective stiffness corresponding to the other frames parallel to it. Fig. 5 (b) represents the idealized model of the 10-storey structure, with masses concentrated for each level, and with effective stiffness between two consecutive stories, which represents the force required to produce a unit displacement [25].

The constitutive values of the springs of the structure (which are given by the lateral stiffness of each floor and shown in Fig. 5 (b)), were obtained as the effective stiffness of all columns between two consecutive levels (assuming that the soil are infinitely stiff). The total effective stiffness for each floor is calculated by the following expression:

$$
k_e = 12 \sum_{i=1}^{nc} \frac{E_c I_i}{L_i}
$$

where, k_e is the effective stiffness of the floor i, nc is the number of columns between every two consecutive levels, E_c is the modulus of elasticity of concrete, L_i is the length of the columns at the $i-th$ level, and I_i is the area moment of inertia of the section of the
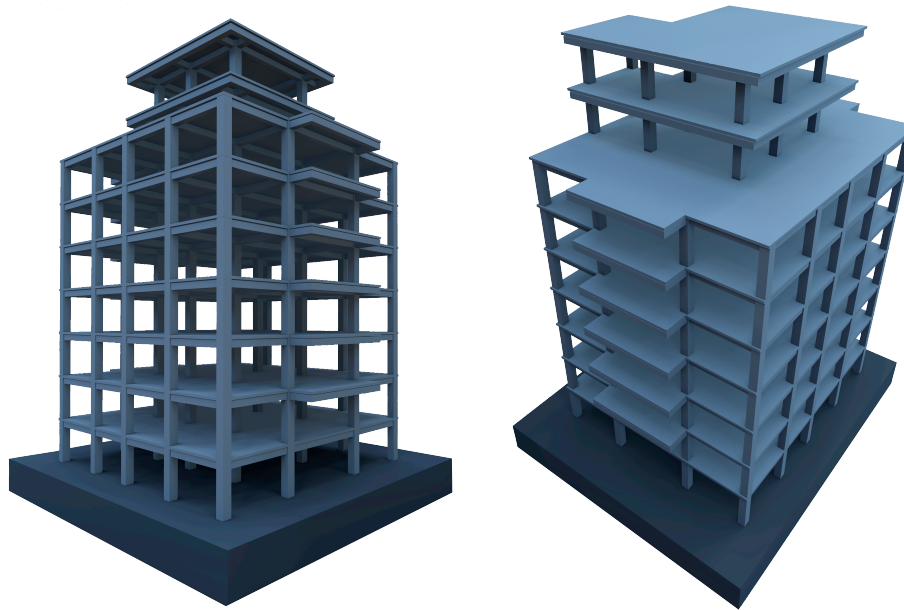
Fig. 4. 10-storey building with reinforced concrete frames and a stiff plate foundation.

columns at the $i - th$ level. The ground stiffness for both k_{sh} and k_{sv} is calculated as an axial stiffness given by $k_s = E_s L_c$, where E_s is the modulus of elasticity of the soil, and L_c is the length of the foundation soil in the N-S direction.

The damping constants of the structure c_i and of the soil c_{sh} and c_{sv} were obtained as constants proportional to the stiffness, through the following expression [25]:

$$c_s = 2\xi m_i \sqrt{\frac{k_i}{m_i}}$$

where, ξ represents the percentage of critical damping, using 5% for reinforced concrete, while for the horizontal and vertical ground damping we assumed 10% [26]. The concentrated masses were calculated for each floor by adding its own weight and the corresponding dead and live loads, according to the geometry and usage of the building. The parameters of the 10-storey building to be analyzed according to the model in Fig. 1 (b) are detailed in Table 1 below.

Table 1. Parameters of the 10-storey building

Level	Floor	L_i (ft)	Mass m_i (lbs)	Stiffness k_i (lb/ft)	Damping coefficient (c_i)
0.00	1	47.49	71,051.75		
13.12	2	13.12	44,131.75	1.54E+08	2.34E+05
26.24	3	13.12	44,131.75	1.54E+08	2.34E+05
39.36	4	13.12	44,131.75	1.54E+08	2.34E+05
52.48	5	13.12	42,578.63	8.71E+07	1.72E+05
65.60	6	13.12	42,578.63	8.71E+07	1.72E+05
78.72	7	13.12	42,004.72	6.50E+07	1.47E+05
91.84	8	13.12	42,004.72	6.50E+07	1.47E+05
101.68	9	9.84	15,591.22	2.97E+07	5.97E+04
111.52	10	9.84	14,120.56	2.97E+07	5.59E+04

Table 2 gives the characteristics of the foundation soil.

Table 2. Bearing ground parameters

USCS Classification:	GW-GC	
Elasticity Module E_s:	73.099,15	lb/ft^2
Horizontal Soil Stiffness k_{sh}:	6.49E+06	lb/ft
Vertical Soil Stiffness k_{sv}:	6.49E+06	lb/ft
Damping Coefficient c_{sh}:	1.40E+05	
Damping Coefficient c_{sv}:	1.40E+05	

For the numerical application of the model, the building will be subjected to a real seismic excitation. The seismic acceleration is applied to the base of the structure. To apply the seismic record to our model, the right-hand term of the equation (13), $f(t)$,
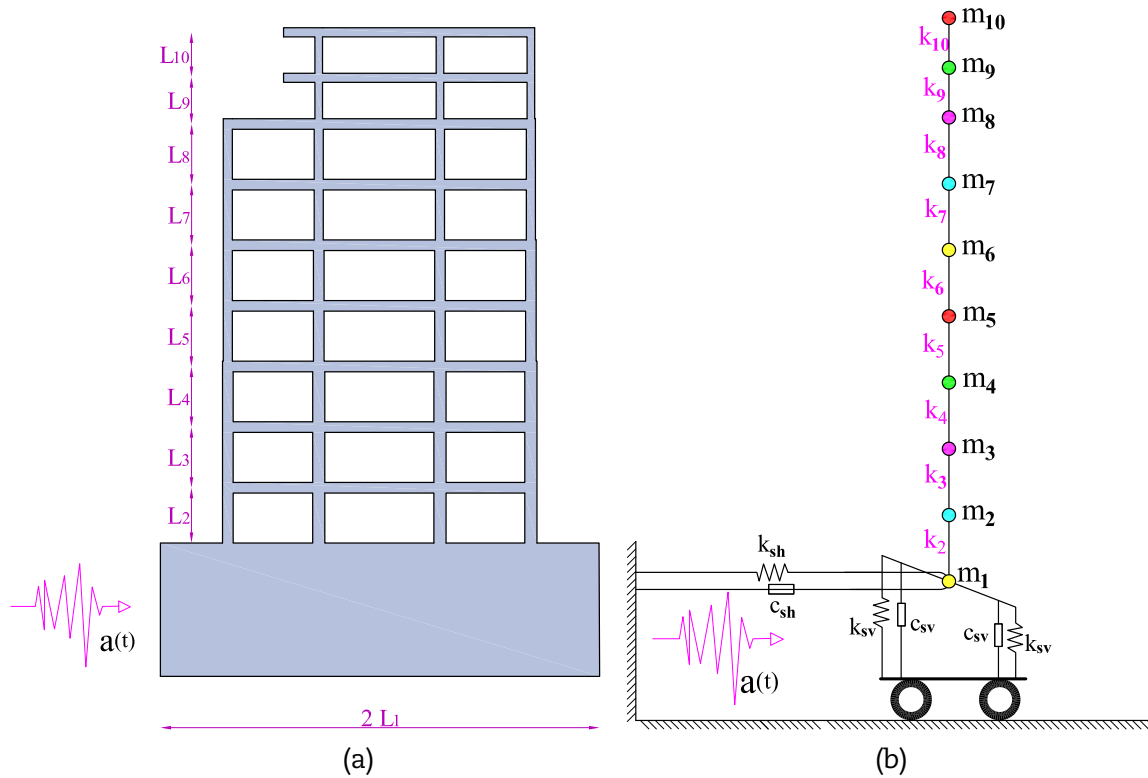
Fig. 5. Equivalent system of concentrated masses: a) plane portal frame of a real 10-story building of which its effective physical and geometrical parameters such as column stiffnesses, inertia of the column cross-sections, floor heights, slab masses, and dampings are listed in Table 1, b) physical-mathematical stick-ball model equivalent to the plane portal frame of the 10-story building in where the masses of the slabs and stiffnesses of the floors are "concentrated", and to which an excitation (of magnitude 7.8Mw) is applied by means of its base.

is given by the product of the total mass of the building $\left(\sum_{i=1}^{n} m_i \right)$ and the acceleration of the earthquake at each time step. As a result, the proposed model determines the position of each of the masses at each time step, resulting from the action of the seismic acceleration.

In this example, the seismic record obtained from the National Network of Accelerographs of Ecuador RENAC (Red Nacional de Acelerógrafos) [27] is used, specifically from the APED N-S station in Pedernales. The magnitude of the earthquake was 7.8 Mw and the hypocenter was located in front of Pedernales (Manabí), 20 km deep [28].

The processing of the acceleration seismic record data was performed with the support of PRISM software, which is freely available for the analysis of the seismic response of single degree-of-freedom systems, developed by the engineering department of INHA University, South Korea [29]. The corrected acceleration and velocity seismic record of the Pedernales earthquake is shown in Fig. 6

6.1 Results

First, a simulation of the building in Fig. 4 being forced by the Pedernales seismic event (see Fig. 6), with the characteristics of both the structure and the soil described in Tables 1 and 2. The results shown in Fig. 7, both for the linear model and for the nonlinear model.

Table 3 summarizes the maximum values of each floor of both the nonlinear model and the linear model, and the percentage difference of the two models for each degree of freedom.

Table 3. Maximum values of the displacements of each floor for nonlinear and linear models

FLOOR	LINEAR MAX DISP.	NON LINEAR MAX DISP.	DIFFERENCE
1	0.570 ft	0.570 ft	0.06
2	0.261 °	0.262 °	0.17
3	0.718 °	0.721 °	0.38
4	0.662 °	0.663 °	0.07
5	0.920 °	0.921 °	0.04
6	0.894 °	0.894 °	0.00
7	1.320 °	1.321 °	0.07
8	1.076 °	1.080 °	0.37
9	2.464 °	2.473 °	0.33
10	1.763 °	1.767 °	0.26

From Figure 7 and Table 3, note that the results of the nonlinear model and the linear model are very similar with differences in the order of 0.38%.
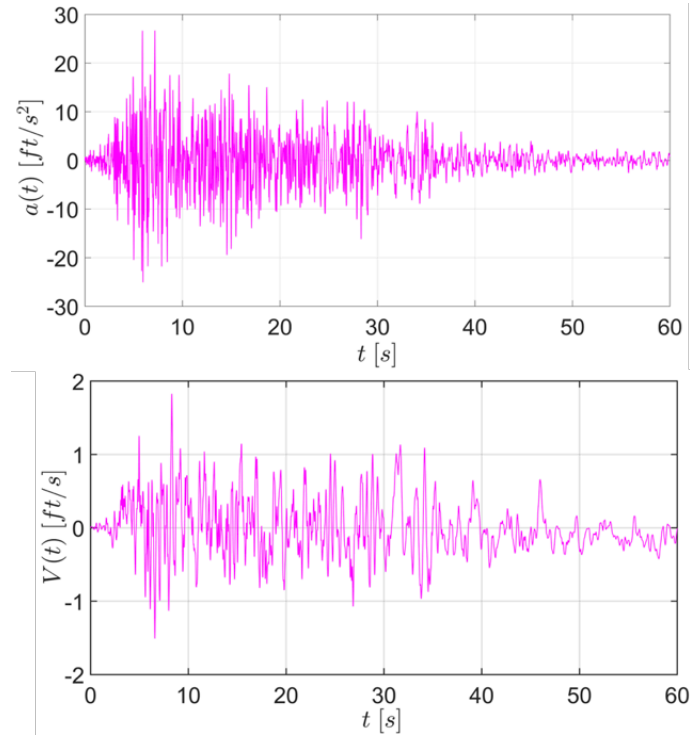
Fig. 6. Velocities and accelerations recorded in the Pedernales earthquake, 2016, Ecuador, magnitude 7.8 Mw, at 27 km depth.

(a) Degree of freedom θ_1

(b) Degree of freedom θ_4

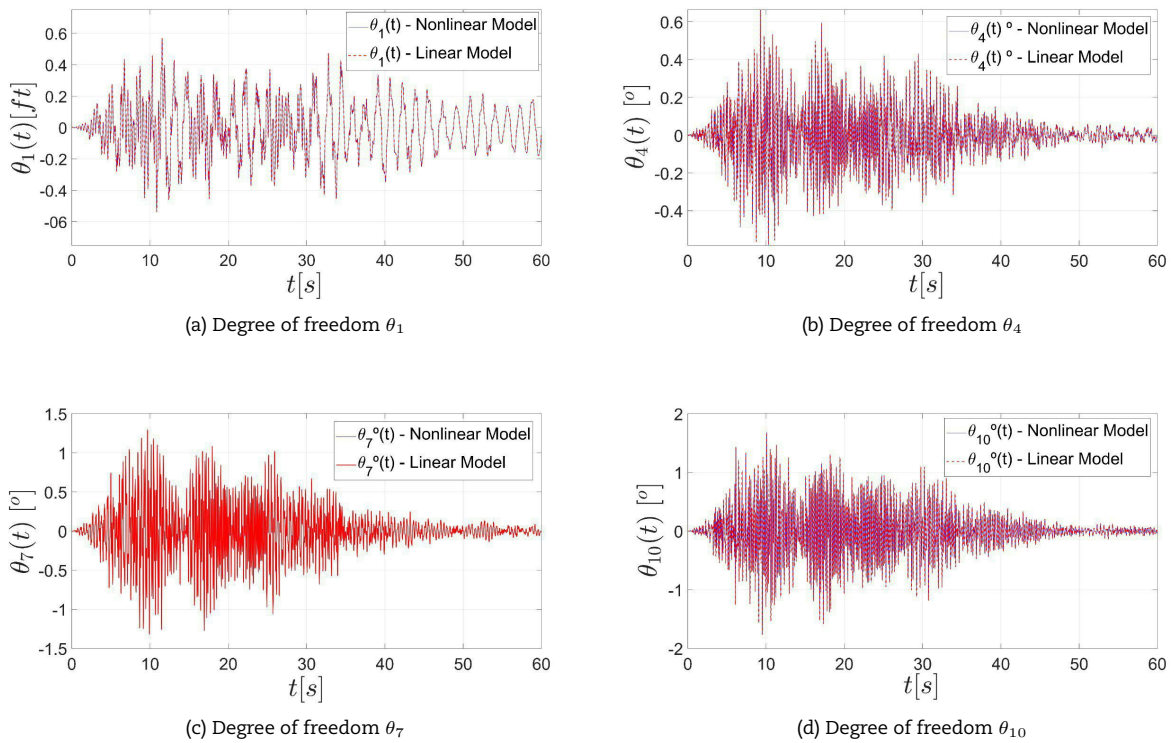(c) Degree of freedom θ_7

(d) Degree of freedom θ_{10}

Fig. 7. Trajectories $\theta_i(t)$ for $i = 1, 4, 7, 10$ (building in Fig. 4) when subjected to the recorded seismic acceleration of the Pedernales earthquake, Ecuador, 2016.
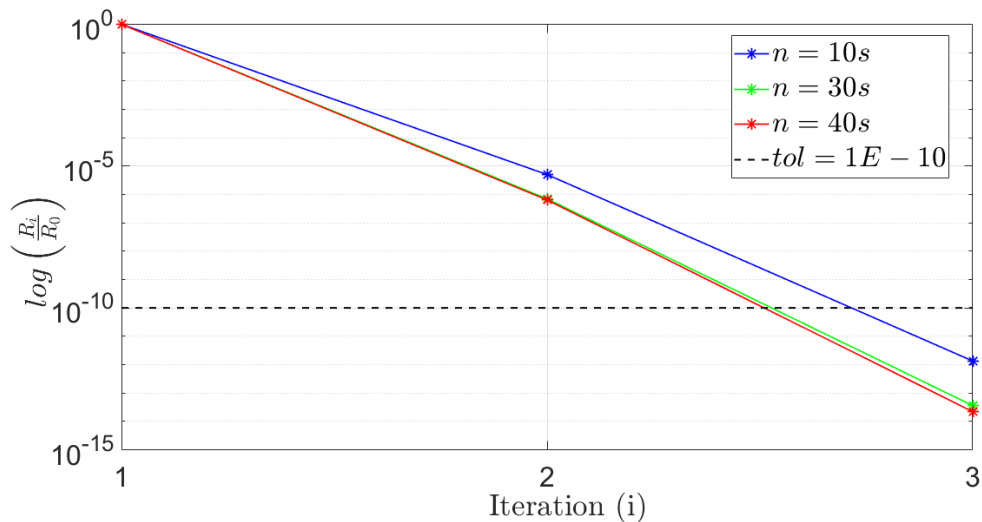
Fig. 8. Convergence of Newton-Raphson method at different time steps: $n = 10s$; $n = 30s$ y $n = 40s$, with a tolerance of $1E - 10$.

In addition, the convergence of the Newton-Raphson method is shown in Fig. 8, where the method converges in three iterations for each of the analyzed time steps, i.e., it has a quadratic convergence, as expected.

6.2 Results by reducing the stiffness values

A second simulation is performed for the 10-storey building in Fig. 4 in which the same parameters are assumed for both the earthquake and the soil characteristics, but reducing the value of the stiffness of each floor to one tenth, obtaining the results seen in Fig. 9.

Table 4 summarizes the maximum values for each floor of both the nonlinear and linear models and the percentage difference of the two models for each degree of freedom.

Table 4. Maximum displacement values of each floor for nonlinear and linear models

FLOOR	LINEAR MAX DISP.	NON LINEAR MAX DISP.	DIFFERENCE
1	1.150 ft	1.154 ft	0.31
2	0.252 °	0.244 °	2.93
3	3.557 °	3.098 °	14.83
4	3.509 °	3.491 °	0.52
5	4.484 °	5.110 °	12.26
6	3.820 °	3.951 °	3.32
7	9.046 °	8.968 °	0.87
8	6.357 °	6.342 °	0.24
9	15.110 °	15.228 °	0.77
10	12.894 °	12.683 °	1.65

Similarly, from Fig. 9 and Table 4, the results of the nonlinear model and the linear model (with reduced stiffness values) begin to have significant differences of up to 14.83%.

6.3 Results subject to initial conditions

A third test of the model is performed using the same parameters of the 10-storey building in Fig. 4 and Table 1 but this time, without external forces (earthquake), but only subjecting the system to initial conditions: initial displacement of 15ft and initial velocity of 6 ft/s, obtaining the results in Fig. 4 and Table 1, obtaining the results in Fig. 10.

Table 5 summarizes the maximum displacement values for each floor of both the nonlinear model and the linear model and the percentage difference of the two models.

In this case, the differences in the application of the linear and nonlinear method are in the order of 0.89% (see Fig. 10 and Table 5).

7. Conclusions

A physical-mathematical model has been presented to determine the deformations of plane frames for any number of floors subjected to an external force at their base, such as, for example, an earthquake. The model considers the geometric nonlinearity of the system due to large deformations or displacements that can be produced by seismic events of considerable magnitude. In addition, the model considers the interaction of the soil with the structure through a system of springs and dampers, both horizontally and vertically, generating a better approximation of the kinematic behavior of the structure.

The model is based on a powerful tool for modeling mechanical phenomena such as the theory of Lagrangian mechanics, through which a nonlinear model for n number of floors is obtained. Once the differential equations are determined, the finite difference

(a) Degree of freedom θ_1

(b) Degree of freedom θ_4

(c) Degree of freedom θ_7

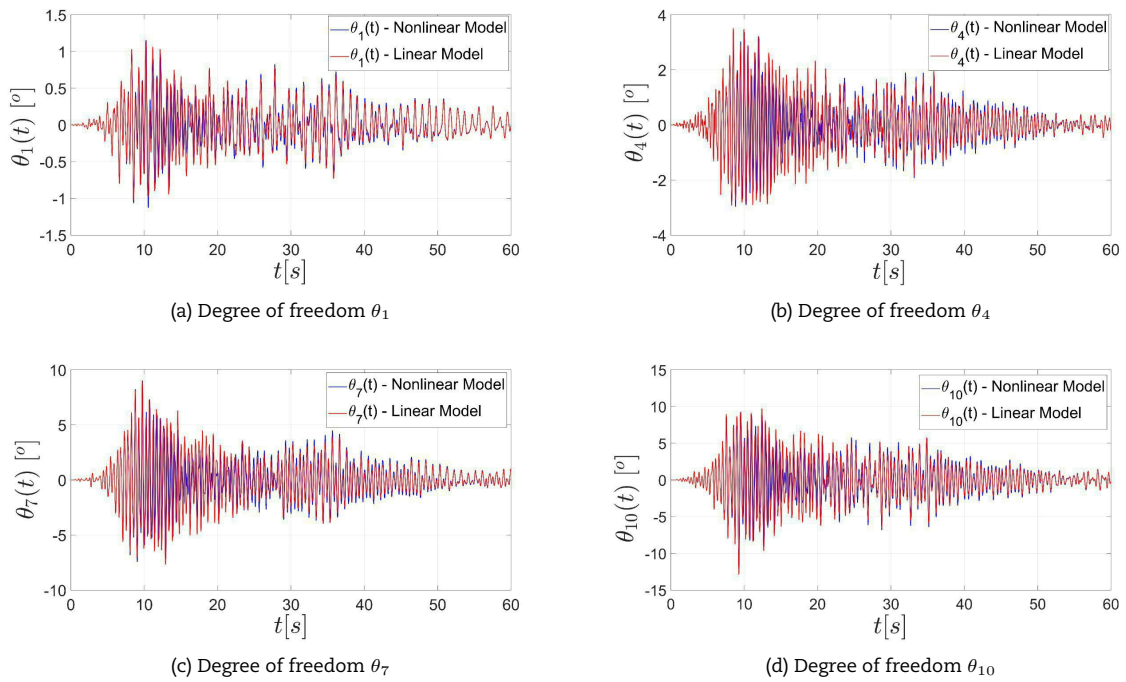(d) Degree of freedom θ_{10}

Fig. 9. Trajectory of the degrees of freedom of the building in Fig. 4 subjected to the reported seismic excitation of the Pedernales earthquake, Ecuador, 2016. Here, the stiffness values have been reduced to ten percent of the original stiffness values of Table. 1
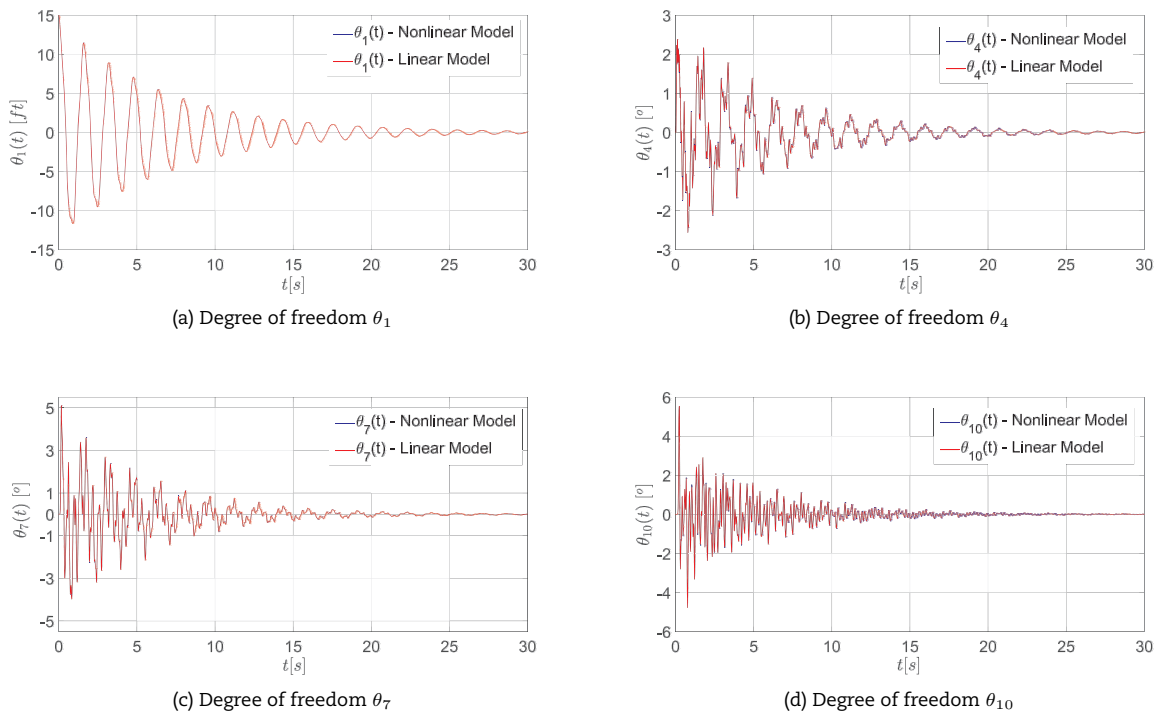

(a) Degree of freedom θ_1

(b) Degree of freedom θ_4

(c) Degree of freedom θ_7

(d) Degree of freedom θ_{10}

Fig. 10. Trajectory of the degrees of freedom of the building in Fig. 4 subject to initial conditions.

Table 5. Maximum displacements values of each floor for the nonlinear and linear model.

FLOOR	LINEAR MAX DISP.	NON LINEAR MAX DISP.	DIFFERENCE
1	15.060 ft	15.060 ft	0.00
2	1.343 °	1.343 °	0.04
3	2.780 °	2.785 °	0.16
4	2.571 °	2.564 °	0.25
5	4.076 °	4.072 °	0.09
6	4.028 °	4.023 °	0.11
7	5.106 °	5.118 °	0.23
8	4.596 °	4.588 °	0.18
9	8.284 °	8.332 °	0.57
10	5.546 °	5.497 °	0.89

numerical method is applied for their numerical solution, generating a system of n nonlinear algebraic equations with n unknowns (once the initial conditions of the phenomenon are taken into account) which is finally solved by the Newton-Raphson method.

In addition, the model is tested by applying it to a real 10-story building, where it is observed that for large stiffnesses, with which buildings are usually designed, the solution of the nonlinear model is very similar to the solution obtained by linearizing the model. However, for smaller stiffnesses, in fact, it is observed that when considering the nonlinearity there are considerable differences with respect to the linear model.

The generalization of the system allows the kinematic analysis of plane building frames of any height and material, considering the geometric nonlinearity produced by large deformations, which can be of great help for an effective pre-dimensioning in the design of structures.

Author Contributions

O.S. Rojas developed the physical-mathematical model and implemented it in MATLAB. A.X. Jerves developed the physical-mathematical model, contributed in the analysis of results and the manuscript edition. D.A. Medina edited the manuscript and contributed in the analysis of results. The manuscript was written through the contribution of all authors. All authors discussed the results, reviewed, and approved the final version of the manuscript.

Acknowledgments

Conflict of Interest

The authors declared no potential conflicts of interest concerning the research, authorship, and publication of this article.

Funding

Data Availability Statements

The datasets generated and/or analyzed during the current study are available from the corresponding author on reasonable request.

References

[1] Chalah-Rezgui, L., Chalah, F., Falek, K., Bali, A. & Nechnech, A., Transverse vibration analysis of uniform beams under various ends restraints. *APCBEE procedia*, 9, 2014, 328–333.

[2] Heng, P., Simplified mechanical models for the Nonlinear Dynamic Analysis of Elasto-plastic steel structures impacted by a rigid body. Ph. D. Thesis, KTH Royal Institute of Technology, Stockholm, SE, 2017.

[3] Chopra, A.K., *Dynamics of structures: theory and applications to earthquake engineering.* Prentice Hall, New Jersey, 1997.

[4] Whitman, V.R., & Richart Jr., F.E., Design procedures for dynamically loaded foundations. *Journal of the Soil Mechanics and Foundations Division* 93(6), 1967, 169–193.

[5] Gutierrez, J.A. & Chopra, A.K., A substructure method for earthquake analysis of structures including structure-soil interaction. John Wiley & Sons, New York,1978.

[6] Bielak, J. & Christiano, P., On the effective seismic input for non-linear soil-structure interaction systems. John Wiley & Sons, New York, 1984

[7] Kenyon, J. M., Non-linear analysis of reinforced concrete plane frames. Ph. D. Thesis, Department of Civil and Environmental Engineering, University of Adelaide, Adelaide, AUS, 1993.

[8] García, F., Comportamiento dinámico de medios poroelásticos en relación con problemas de interacción suelo-estructura y suelo-agua-estructura, Ph.D. Thesis,International Journal of soil dynamics and earthquake engineering, Gran Canarias, ESP, 2012.

[9] Cadena P., J.M. and others, Two-dimensional lagrangian model for nonlinear soil-structure interactions, B.S. Thesis, Universidad San Francisco de Quito, Quito, ECU, 2017.

[10] Rosson, B.T., A virtual work approach to modeling the nonlinear behavior of steel frames. *Journal of Civil Engineering and Architecture*, 12(5), 2018, 323-334.

[11] Habibi, A., & Bidmeshki, S., A dual approach to perform geometrically nonlinear analysis of plane truss structures. *Steel and composite structures*, 27(1), 2018, 13-25.

[12] de Araujo, F.C., Ribeiro, I.S., & Silva, K.I., Geometric nonlinear analysis of plane frames with generically nonuniform shear-deformable members. *Structures*, 12, 2017, 179-187.

[13] Greco, A., Caddemi, S., Caliò, I., Fiore, I., A Review of Simplified Numerical Beam-like Models of Multi-Storey Framed Buildings. *Buildings*, 12(9), 1397, 2022.

[14] Izzuddin, B. A., Nonlinear dynamic analysis of framed structures. Ph. D. Thesis, University of London, London, ENG, 1990.
[15] Turco, E., Barchiesi, E., Giorgio, I., & dell'Isola, F., A Lagrangian Hencky-type non-linear model suitable for metamaterials design of shearable and extensible slender deformable bodies alternative to Timoshenko theory. *International Journal of Non-Linear Mechanics*, 123, 2020.
[16] Gazetas, G., Analysis of machine foundation vibrations: state of the art *International Journal of soil dynamics and earthquake engineering*, Elsevier, 1, 1983, 2-42.
[17] Wolf, J.P., Earthquake engineering & structural dynamics: Spring-dashpot-mass models for foundation vibrations, John Wiley & Sons, New York, 1997.
[18] Pender, M.J., Earthquake-soil structure interaction, spring and dashpot models, and real soil behaviour. *IBulletin of the New Zealand Society for Earthquake Engineering*, 4, 1983, 320-330.
[19] Serra-Aguila, A., Puigoriol-Forcada, J.M. Reyes, G. & Menacho, J., Viscoelastic models revisited: characteristics and interconversion formulas for generalized Kelvin–Voigt and Maxwell models, Springer, 6, 2019, 1191-1209.
[20] Agila, A., Baleanu, D., Eid, R., & Irfanoglu, B., Applications of the extended fractional Euler-Lagrange equations model to freely oscillating dynamical systems. *Rom. J. Phys*, 61, 2016, 350-359.
[21] Fetecau, R.C., Marsden, J.E., Ortiz, M. & West, M., Nonsmooth Lagrangian mechanics and variational collision integrators. *SIAM Journal on Applied Dynamical Systems*, 3, 2003, 381-416.
[22] Taylor, J.R., *Classical mechanics*. University Science Book, California, 2005.
[23] Jerves, A.X., *Elementos de Cálculo Numérico*. Editorial Universitaria UTE, Quito, 2021.
[24] Deuflhard, P., *Newton methods for nonlinear problems: affine invariance and adaptive algorithms*. Springer Science & Business Media, Berlín, 2005.
[25] Chopra, A.K., *Dynamics of structures*. Pearson Prentice Hall, New Jersey, 2012.
[26] Priestley, M.J.N. & Grant, D.N., Viscous damping in seismic design and analysis. *International Journal of Non-Linear Mechanics*, 9, 2005, 229–255.
[27] Falconi, R.A., Peligrosidad sísmica de la costa norte de Ecuador y el terremoto de Pedernales de 2016. *Revista Geofísica*, 67, 2017, 9-24.
[28] Toulkeridis, T., Chunga, K., Rentería, W., Rodriguez, F., Mato, F., Nikolaou, S., Antonaki, N., Diaz-Fanas, G., Besenzon, D. & otros, Mw 7.8 Muisne, Ecuador 4/16/16 observaciones del terremoto: agrupamiento geofísico, mapeo de intensidad, tsunami. *Proc. 16ª Conferencia Mundial sobre Ingeniería Sísmica, 16WCEE*, Muisne, Ecuador, 1-10, 2017.
[29] Jeong, S.H., Lee, K.H. & Jang, W.S., PRISM for earthquake engineering. *Dept. of Architectural Engineering*, INHA University, Incheon, South Korea, 2016.

ORCID iD

Omar S. Rojas https://orcid.org/0000-0003-2972-3408
Alex X. Jerves https://orcid.org/0000-0002-6556-8727
David A. Medina https://orcid.org/0000-0001-5219-0828

Publisher's Note Shahid Chamran University of Ahvaz remains neutral with regard to jurisdictional claims in published maps and institutional affiliations.